Inorg. Chem. **2008**, *47*, 10729−10738

Factors Influencing Tetranuclear [2 × 2] Grid vs Dinuclear Side-by-Side Structures for Silver(I) Complexes of Pyridazine-Based Bis-Bidentate Ligands

Jason R. Price,[†] Nicholas G. White,[†] Alejandro Perez-Velasco,[§] Geoffrey B. Jameson,[‡] Christopher A. Hunter,[§] and Sally Brooker*[,†]

Department of Chemistry and MacDiarmid Institute for Advanced Materials and Nanotechnology, University of Otago, P.O. Box 56, Dunedin, New Zealand, Institute of Fundamental Sciences, Chemistry, Massey University, P.O. Box, 11222, Palmerston North, New Zealand, Krebs Institute for Biomedical Science, Department of Chemistry, University of Sheffield, Sheffield, United Kingdom

Received May 27, 2008

Silver(I) complexes of five bis-bidentate Schiff-base ligands, derived from 3,6-diformylpyridazine and substituted anilines (2,4-dimethylaniline $\mathbf{L}^{o,p\text{-Me}}$; 3,5-dichloroaniline $\mathbf{L}^{m,m\text{-Cl}}$; 2-aminobiphenyl $\mathbf{L}^{o\text{-Ph}}$; *p*-toluidine $\mathbf{L}^{p\text{-Me}}$; 4-aminophenol $\mathbf{L}^{p\text{-OH}}$; *p*-anisidine $\mathbf{L}^{p\text{-OMe}}$), have been prepared. The ligands have a wide range of steric and electronic properties due to variation in the extent and nature of the substitution of the aniline rings. Four of the resulting complexes were structurally characterized by X-ray crystallography: three of the four, $[Ag_2(\mathbf{L}^{o,p\text{-Me}})_2](BF_4)_2$, $[Ag_2(\mathbf{L}^{m,m\text{-Cl}})_2](BF_4)_2$ and $[Ag_2(\mathbf{L}^{o\text{-Ph}})_2](BF_4)_2$ formed dinuclear side-by-side complexes, while $[Ag_4(\mathbf{L}^{p\text{-Me}})_4](BF_4)_4$ gave a tetranuclear [2 × 2] grid. The previously reported tetranuclear [2 × 2] grid $[Ag_4(\mathbf{L}^{p\text{-OMe}})_4](BF_4)_4$ was recrystallized in the presence of benzene to see if this would alter the architecture of this complex. It did not: the [2 × 2] grid architecture was retained despite the benzene molecules of solvation. Given the flexibility of silver(I) with regard to coordination geometry, the molecular structure of these complexes is influenced mostly by the ligand rather than the metal ion. In each case, the factors which influence the molecular architecture are presented and discussed. Substituent effects on the electrostatics of the intramolecular ligand−ligand $\pi-\pi$ interactions (XED2.8) account for some of the differences observed in the structures.

Introduction

There is much interest in understanding the mechanisms involved in molecular self-assembly, in order that control may be exerted over these processes. Metal ions are frequently used to direct this self-assembly, and a wide range of interesting molecular architectures has been realized in this manner.[1] Using a metal ion with a clear coordination geometry preference allows reasonable predictions of molecular architecture to be made, as appropriately designed ligands can be expected to organize themselves in a fairly predictable manner around the metal ion to fit this favored geometry. However, if metal ions with more plastic coordination geometries are utilized, the influence of the preferred coordination geometry of the metal ion becomes less important as a range of geometries can be relatively readily accommodated, and instead ligand-centered factors are key with regard to determining the architecture and properties of the resulting complex. Ligand-centered factors may include steric and electronic properties, and/or may involve intramolecular and intermolecular effects such as π-π and anion (strictly π*-anion) interactions, and hydrogen bonding.

We have previously shown that the ligand $\mathbf{L}^{p\text{-OMe}}$ (Figure 1) can form either a dinuclear side-by-side complex by using a first-row transition metal ion that prefers an octahedral

* To whom correspondence should be addressed. Tel: +64 3 479 7919. Fax: +64 3 479 7906. E-mail: sbrooker@chemistry.otago.ac.nz.
[†] University of Otago.
[§] University of Sheffield.
[‡] Massey University.

(1) Ruben, M.; Rojo, J.; Romero-Salguero, F. J.; Uppadine, L. H.; Lehn, J.-M. *Angew. Chem., Int. Ed.* **2004**, *43*, 3644–3662.

(2) Lan, Y.; Kennepohl, D. K.; Moubaraki, B.; Murray, K. S.; Cashion, J. D.; Jameson, G. B.; Brooker, S. *Chem. Eur. J.* **2003**, *9*, 3772–3784, and front cover feature.

10.1021/ic800959s CCC: $40.75
Published on Web 10/21/2008

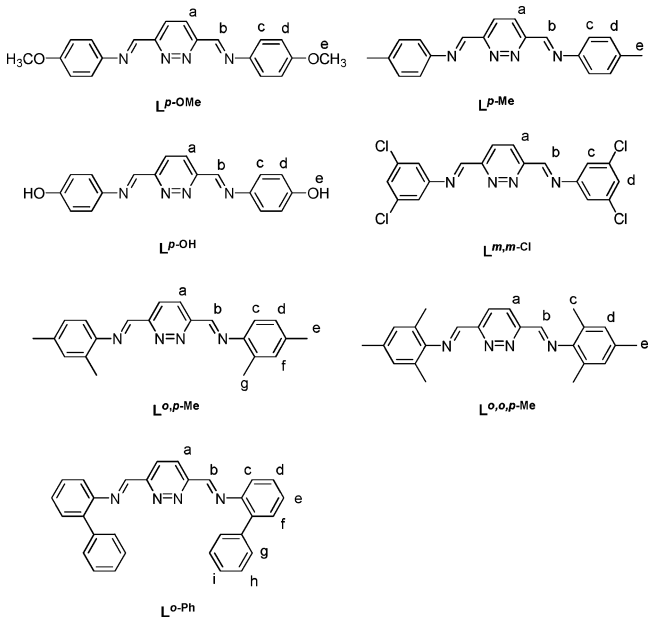

Figure 1. The acyclic Schiff base ligands, derived from the condensation of 3,6-diformylpyridazine with 2 equiv of the appropriately substituted aniline derivative, employed in this study.

Scheme 1[a]

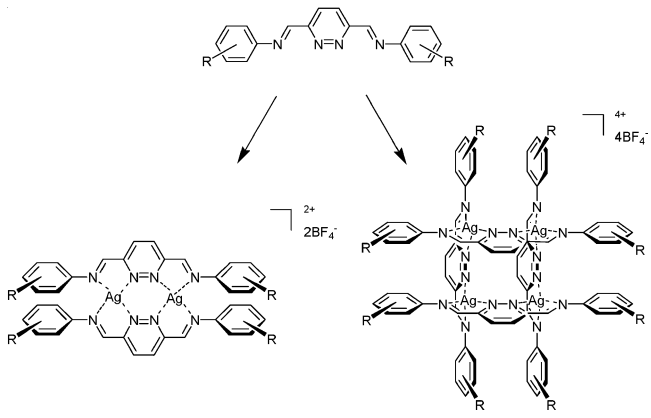

[a] Reagents and conditions: 3 h reflux, nitromethane.

geometry or a [2 × 2] grid complex by using copper(I) ions, which prefer a tetrahedral geometry.[2] Further studies using a range of related, acyclic, bis-bidentate ligands (readily prepared by the 1:2 Schiff base condensation of 3,6-diformylpyridazine and commercially available substituted anilines) (Figure 1) and copper(I) ions showed that [2 × 2] tetranuclear grids formed unless the twisted ligand $\mathbf{L}^{o\text{-Ph}}$ was used, in which case a dinuclear side-by-side architecture was observed (Scheme 1).[3] The formation of such grid architectures is facilitated by the use of planar ligands. For this ligand family, when non-sterically demanding substitution patterns are present, a planar conformation is the preferred ligand arrangement, as observed crystallographically,[3] because it allows conjugation throughout the entire ligand strand. On the other hand, if substituents are added to the phenyl ring at positions *ortho* to the imine group, these are sterically demanding and force a rotation around the imine-phenyl

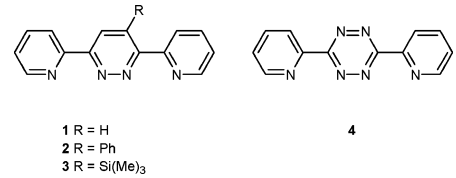

Figure 2. The 3,6-dipyridylpyridazine and 3,6-dipyridyltetrazine ligands used by the groups of Constable and Dunbar.[5–10]

bond. Although this disrupts the conjugation throughout the ligand, the steric strain is reduced. Twisted ligands like this are not optimal for grid formation as forming a grid would push the phenyl rings on adjacent ligand strands into one another, but they are nicely preorganized for side-by-side complex formation where such a twist is a requirement for the two ligands to sandwich two metal ions without the phenyl rings clashing with each other.

In contrast to copper(I), silver(I) ions adopt a tetrahedral geometry much less readily.[4] Indeed, silver(I) ions are known to adopt numerous and varied coordination geometries, and prediction of the structures of self-assembled complexes of silver(I) is therefore extremely difficult.[5] For example, the closely related ligands **1**−**4** (Figure 2) have resulted in complexes in which the silver(I) ions adopt pseudo-tetrahedral,[5,6] pseudo-square planar,[6−9] trigonal planar,[10] and trigonal prismatic[5,6] geometries. The geometric flexibility of silver(I) makes it an ideal metal ion to examine in more detail the ways in which *ligands*, or *anions*,[6] may be used to control the molecular architecture of metallosupramolecular assemblies, instead of the more conventional approach of using the metal ion to control structure. We therefore decided to examine the architectures of the silver(I) complexes of the family of pyridazine-based bis-bidentate ligands shown in Figure 1, holding the anion constant so as to remove that factor from consideration.

In a previous communication we reported the synthesis of the 1:1 silver(I):$\mathbf{L}^{p\text{-OMe}}$ complex and its single crystal X-ray structure, only the second tetrasilver(I) [2 × 2] grid to be so characterized[11] (the first having been reported by Lehn and co-workers in 2005 ref 12). In addition, through the introduction of sterically demanding *ortho*-methyl substituents on the phenyl rings, that is, the use of the very twisted ligand $\mathbf{L}^{o,o,p\text{-Me}}$, we were able to preorganize the ligand to facilitate access to a disilver(I) side-by-side architecture {the steric demands of the ligand presumably

(3) Price, J. R.; Lan, Y.; Brooker, S. *Dalton Trans.* **2007**, 1807–1820.
(4) Greenwood, N. N.; Earnshaw, A., *Chemistry of the Elements*, 1st ed.; Pergamon Press: Exeter, 1984; p 1315.
(5) Schottel, B. L.; Bacsa, J.; Dunbar, K. R. *Chem. Commun.* **2005**, 46–47.
(6) Schottel, B. L.; Chifotides, H. T.; Shatruk, M.; Chouai, A.; Pérez, L. M.; Bacsa, J.; Dunbar, K. R. *J. Am. Chem. Soc.* **2006**, *128*, 5895–5902.
(7) Constable, E. C.; Housecroft, C. E.; Kariuki, B. M.; Neuburger, M.; Smith, C. B. *Aust. J. Chem.* **2003**, *56* (7), 653–655.
(8) Constable, E. C.; Housecroft, C. E.; Kariuki, B. M.; Kelly, N.; Smith, C. B. *C. R. Chimie* **2002**, *5*, 425–430.
(9) Constable, E. C.; Housecroft, C. E.; Kariuki, B. M.; Kelly, N.; Smith, C. B. *Inorg. Chem. Commun.* **2002**, (5), 199–202.
(10) Constable, E. C.; Housecroft, C. E.; Neuburger, M.; Reymann, S.; Schaffner, S. *Chem. Commun.* **2004**, (9), 1056–1057.
(11) Price, J. R.; Lan, Y.; Jameson, G. B.; Brooker, S. *Dalton Trans.* **2006**, 1491–1494, and front cover feature.
(12) Patroniak, V.; Stefankiewicz, A. R.; Lehn, J.-M.; Kubicki, M. *Eur. J. Inorg. Chem.* **2005**, 4168–4173.

Table 1. Crystal Structure Determination Details for the Complexes $[Ag^{I}_2(\mathbf{L}^{o,p\text{-Me}})_2](BF_4)_2 \cdot 2CH_3NO_2$, $[Ag^{I}_4(\mathbf{L}^{p\text{-OMe}})_4](BF_4)_4 \cdot 1.5C_6H_6 \cdot$solvent, $[Ag^{I}_4(\mathbf{L}^{p\text{-OMe}})_4](BF_4)_4 \cdot 4.2(CH_3)_2NCHO \cdot 0.8(C_2H_5)_2O$, $[Ag^{I}_2(\mathbf{L}^{m,m\text{-Cl}})_2](BF_4)_2 \cdot 2CH_3NO_2 \cdot C_6H_6$, $[Ag^{I}_2(\mathbf{L}^{o\text{-Ph}})_2](BF_4)_2$

	$[Ag^{I}_2(\mathbf{L}^{o,p\text{-Me}})_2]^{2+}$	$[Ag^{I}_4(\mathbf{L}^{p\text{-OMe}})_4]^{4+}$	$[Ag^{I}_4(\mathbf{L}^{p\text{-Me}})_4]^{4+}$	$[Ag^{I}_2(\mathbf{L}^{m,m\text{-Cl}})_2]^{2+}$	$[Ag^{I}_2(\mathbf{L}^{o\text{-Ph}})_2]^{2+}$
empirical formula	$C_{45}H_{47}Ag_2B_2F_8N_9O_2$	$2[C_{89}H_{81}Ag_4B_4F_{16}N_{16}O_8]$	$C_{95.8}H_{109.4}Ag_4B_4F_{16}N_{20.2}O_5$	$C_{44}H_{32}Ag_2B_2Cl_8F_8N_{10}O_4$	$C_{60}H_{44}Ag_2B_2F_8N_8$
M_r	1135.28	4562.84	2402.56	1437.76	1266.39
crystal system	monoclinic	monoclinic	triclinic	triclinic	monoclinic
space group	*C*2/*c*	*C*2/*c*	$P\bar{1}$	$P\bar{1}$	*P*2/*c*
a [Å]	26.757(18)	60.305(3)	13.6114(6)	7.2637(14)	29.610(6)
b [Å]	11.094(7)	21.3256(10)	18.7137(8)	10.339(2)	12.576(3)
c [Å]	15.482(11)	46.174(3)	21.0146(9)	36.685(8)	14.106(3)
α [°]	90	90	78.652(2)	97.592(4)	90
β [°]	91.942(6)	130.615(6)	85.772(2)	93.876(4)	103.68(3)
ν [°]	90	90	81.763(2)	96.874(4)	90
V [Å^3]	4593(5)	45076(4)	5188.3(4)	2701.6(10)	5103.7(19)
Z (*Z*′, cryst symm)	4 (2 × 1/2, −1)	8 (1)	2 (1)	2 (2 × 1/2, −1)	4 (2 × 1/2, 2)
ν_{calcd} [g/cm^3]	1.642	1.345	1.552	1.767	1.648
μ [mm^{-1}]	0.935	0.765	0.834	1.201	0.848
F(000)	2288	18288	2435	1420	2544
crystal size [mm]	0.75 × 0.12 × 0.10	0.40 × 0.22 × 0.16	0.16 × 0.14 × 0.04	0.40 × 0.10 × 0.02	0.20 × 0.20 × 0.16
θ range for data collection [°]	1.99 to 26.40	2.92 to 21.97	0.99 to 26.00	2.00 to 26.41	2.80 to 26.37
reflections collected	19287	295222	115563	19908	96210
independent reflections	4679	27431	20363	10517	10422
R(int)	0.0402	0.0869	0.1125	0.1130	0.0492
max and min transmission	1.000 and 0.825	1.000 and 0.736	1.000 and 0.801	1.00 and 0.75	1.00 and 0.640
data/restraints/parameters	4679/0/313	27431/2345/2401	20363/128/1394	10517/0/705	10422/429/752
GOF (F^2)	1.024	1.020	1.069	0.923	1.076
R_1 [$I > 2\sigma(I)$]	0.0267	0.0813	0.0652	0.0644	0.0315
wR_2 [all data]	0.0613	0.2490	0.1590	0.1162	0.1008
comments	no disorder	twinned/squeezed	disorder modeled	no disorder	twinned

disfavored the tetrasilver(I) [2 × 2] grid architecture}. Here, we expand on that study and describe the new 1:1 silver(I) complexes of $\mathbf{L}^{p\text{-OH}}$, $\mathbf{L}^{p\text{-Me}}$, $\mathbf{L}^{o,p\text{-Me}}$, $\mathbf{L}^{o\text{-Ph}}$, and $\mathbf{L}^{m,m\text{-Cl}}$, along with further results relating to the silver(I) complex of $\mathbf{L}^{p\text{-OMe}}$. Within this series of ligands the degree of electron donation or withdrawal by the phenyl ring substituents is varied. In addition, the extent of steric hindrance, which when present in the ligand at the *ortho*-phenyl sites is expected to reduce the planarity and hence the extent of conjugation, has been varied. As in our earlier studies, the anion used has been held constant (cf. recent results from Dunbar et al.[5,6,13]), BF_4^-, in order to keep the variables to a minimum. The synthesis and characterization of the products of the 1:1 Ag(I):L reactions are presented and the structural outcomes, tetrasilver(I) [2 × 2] grid vs. disilver(I) side-by-side, are analyzed and discussed.

Experimental Procedures

The $\mathbf{L}^{p\text{-OH}}$,[3] $\mathbf{L}^{p\text{-OMe}}$,[2] $\mathbf{L}^{o,o,p\text{-Me}}$, $\mathbf{L}^{p\text{-Me}}$, $\mathbf{L}^{o,p\text{-Me}}$, $\mathbf{L}^{o\text{-Ph}}$, and $\mathbf{L}^{m,m\text{-Cl}}$ ligands[3] and the $[Ag_4(\mathbf{L}^{p\text{-OMe}})_4](BF_4)_4$ and $[Ag_2(\mathbf{L}^{o,o,p\text{-Me}})_2](BF_4)_2$ complexes[11] were prepared as described previously. The NMR and IR data for these two complexes are reported below. All measurements were carried out as described previously.[14,15]

Crystal Structure Determinations. Single crystal X-ray diffraction data for $[Ag_2(\mathbf{L}^{o,p\text{-Me}})_2][BF_4]_2 \cdot CH_3NO_2$ (at 101 K) and $[Ag_2(\mathbf{L}^{m,m\text{-Cl}})_2][BF_4]_2 \cdot (C_6H_6) \cdot 2CH_3NO_2$ (at 112 K) were collected on a Bruker SMART CCD diffractometer (University of Canterbury). The data for the other three structures were collected on a Bruker Kappa Apex II area detector diffractometer (University of Otago) at 83 K. In all cases graphite monochromated Mo Kα radiation (λ = 0.71073 Å) was used. All data sets were corrected for absorption using SCALE/SADABS.[16,17] The structures were solved using SHELXS-97 and refined against F^2 using all data by full-matrix least-squares techniques with SHELXL-97.[18] All non-hydrogen atoms were modeled anisotropically except where noted. Hydrogen atoms were inserted at calculated positions and rode on the atoms to which they are attached (including isotropic thermal parameters which were equal to 1.2 times the attached non-hydrogen atom, except for the OMe hydrogens in $[Ag_4(\mathbf{L}^{p\text{-OMe}})_4](BF_4)_2$ where isotropic thermal parameters were equal to 1.5 times the attached carbon). For the structures with partial occupancy and/or disorder, $[Ag_4(\mathbf{L}^{p\text{-Me}})_4](BF_4)_4 \cdot 4.2(DMF) \cdot 0.8(Et_2O)$, $[Ag_4(\mathbf{L}^{p\text{-OMe}})_4](BF_4)_4 \cdot 1.5(C_6H_6) \cdot$solvent and $[Ag_2(\mathbf{L}^{o\text{-Ph}})_2](BF_4)_2$, occupancies were initially freely refined then fixed. Both of the latter two structures are twinned. That of $[Ag_4(\mathbf{L}^{p\text{-OMe}})_4](BF_4)_4 \cdot 1.5(C_6H_6) \cdot$solvent was also subjected to the SQUEEZE routine of PLATON.[19] Full details of the disorder modeling, twinning and SQUEEZE for these three structures are given in the Supporting Information.

Crystal structure determination details are summarized in Table 1. CCDC 680759−680763 contain the supplementary crystallographic data for this paper.

$[Ag_n(\mathbf{L}^{p\text{-OH}})_n](BF_4)_n \cdot {}^n/_3H_2O$. A solution of silver tetrafluoroborate (0.0155 g, 0.079 mmol) in nitromethane (5 mL) was added to a stirred yellow suspension of $\mathbf{L}^{p\text{-OH}}$ (0.0253 g, 0.079 mmol) in nitromethane (20 mL) causing the color to change to orange. The resultant solution was heated at reflux for 3 h, allowed to cool to room temperature, and the orange microcrystalline product that precipitated was removed by filtration (21.7 mg, 53%). Found C, 41.49; H, 2.78; N, 10.97%. $[Ag_n(C_{18}H_{14}N_4O_2)_n](BF_4)_n \cdot {}^n/_3H_2O$ requires: C, 41.66; H, 2.85; N, 10.87. ^{1}H NMR (500 MHz, solvent $(CD_3)_2NCDO$ [dimethylformamide-d_7] δ_H relative to $(CD_3)_2NC\mathbf{H}O$ at 8.02 ppm) 10.36 (2nH, s, H-e), 9.22 (2nH, s, H-b), 8.71 (2nH, s, H-a), 7.45 (4nH, br, H-c,), 6.71 (4nH, br, H-d). IR (KBr disk,

(13) Campos-Fernández, C. S.; Schottel, B. L.; Chifotides, H. T.; Bera, J. K.; Bacsa, J.; Koonen, J. M.; Russell, D. H.; Dunbar, K. R. *J. Am. Chem. Soc.* **2005**, *127*, 12909–12923.
(14) Brooker, S.; Kelly, R. J. *J. Chem. Soc., Dalton Trans.* **1996**, 2117–2122.
(15) Brooker, S.; Davidson, T. C.; Hay, S. J.; Kelly, R. J.; Kennepohl, D. K.; Plieger, P. G.; Moubaraki, B.; Murray, K. S.; Bill, E.; Bothe, E. *Coord. Chem. Rev.* **2001**, *216−217*, 3–30.
(16) Sheldrick, G. M. *SADABS. Empirical Absorption Correction Program for Area Detector Data*: University of Göttingen: Göttingen, 1996.
(17) Blessing, R. H. *Acta Crystallogr., Sect. A* **1995**, *51*, 33–38.
(18) Sheldrick, G. M. *Acta Crystallogr., Sect. A* **2008**, *A64*, 112–122.
(19) van der Sluis, P.; Spek, A. L. *Acta Crystallogr., Sect. A* **1990**, *46*, 194–201.

inter alia) ν_{max}/cm^{-1}: 3456 (s, br), 3076 (m), 2968 (m), 1627 (m), 1588 (vs), 1508 (s), 1446 (m), 1340 (m), 1279 (s), 1174 (s), 1084 (s, br), 851 (s), 835 (m), 576 (m), 530 (m).

$[Ag_4(L^{p\text{-}Me})_4](BF_4)_4\cdot 2H_2O$. A solution of silver tetrafluoroborate (0.0290 g, 0.149 mmol) in nitromethane (5 mL) was added to a stirred yellow suspension of $L^{p\text{-}Me}$ (0.0469 g, 0.149 mmol) in nitromethane (20 mL) causing an immediate color change to blood red. The resulting solution was heated at reflux for 3 h, allowed to cool to room temperature and the volume reduced to ~1/3 under reduced pressure. Diethyl ether vapor was diffused into the reaction solution yielding a red powder which was further purified by diffusion of diethyl ether into a DMF solution of the crude product (24.1 mg, 31%). Found C, 46.46; H, 3.83; N, 11.02%. $[Ag_4(C_{20}H_{18}N_4)_4](BF_4)_4\cdot 2H_2O$ requires: C, 46.37; H, 3.70; N, 10.81%. ^{1}H NMR (500 MHz, solvent, CD_3NO_2 [nitromethane-d_3] δ_H relative to CD_2HNO_2 at 4.33 ppm) 9.09 (8H, d, H-b), 8.59 (8H, s, H-a), 7.27 (16H, d, J = 9 Hz, H-c), 6.93 (16H, d, J = 9 Hz, H-d), 2.087 (24H, s, H-e). ^{13}C NMR (125 MHz, solvent CD_3NO_2 [nitromethane-d_3] δ_c relative to CD_3NO_2 at 62.81 ppm) 155.8, 153.0, 144.0, 143.3, 136.5, 131.9, 125.1, 21.3. IR (KBr disk, inter alia) ν_{max}/cm^{-1}: 3029 (m), 2921 (m), 1654 (m), 1625 (m), 1591 (s), 1505 (m), 1436 (m), 1175 (m), 1063 (vs, br), 963 (m), 908 (m), 812 (s), 571 (m), 521 (m).

$[Ag_2(L^{o,p\text{-}Me})_2](BF_4)_2\cdot CH_3NO_2$. A solution of silver tetrafluoroborate (0.0244 g, 0.125 mmol) in nitromethane (5 mL) was added to a stirred yellow suspension of $L^{o,p\text{-}Me}$ (0.0429 g, 0.125 mmol) in nitromethane (20 mL) causing an immediate color change to blood red. The resulting solution was heated at reflux for 2 h, allowed to cool to room temperature and the volume reduced to ~1/3 under reduced pressure. Diethyl ether vapor was diffused into the reaction solution yielding an orange crystalline solid (50.2 mg, 71%). Found C, 47.66; H, 4.36; N, 11.23%. $[Ag_2(C_{22}H_{22}N_4)_4](BF_4)_2.CH_3NO_2$ requires: C, 47.61; H, 4.17; N, 11.10%. ^{1}H NMR (500 MHz, solvent, CD_3NO_2 [nitromethane-d_3] δ_H relative to CD_2HNO_2 at 4.33 ppm) 8.86 (4H, s, H-b), 8.55 (4H, s, H-a), 7.09 (8H, m, H-c and H-d), 6.60 (4H, s, H-f), 2.33 (12H, s, H-e), 2.08 (12H, s, H-g). ^{13}C NMR (125 MHz, solvent CD_3NO_2 [nitromethane-d_3] δ_c relative to CD_3NO_2 at 62.81 ppm) 158.2, 155.4, 147.2, 140.4, 135.3, 133.1, 132.6, 128.9, 120.2, 21.6, 18.5. IR (KBr disk, inter alia) ν_{max}/cm^{-1}: 3059 (m), 2918 (m), 1622 (m), 1595 (m), 1560 (s), 193 (m), 1432(m), 1407 (m), 1375 (m), 1064 (vs, br), 1027 (vs, br), 899 (m), 827 (m), 814 (s), 717 (m), 663 (m), 571 (m), 520 (m).

$[Ag_2(L^{o\text{-}Ph})_2](BF_4)_2\cdot CH_3NO_2\cdot H_2O$. A solution of silver tetrafluoroborate (0.0239 g, 0.123 mmol) in nitromethane (5 mL) was added to a stirred yellow suspension of $L^{o\text{-}Ph}$ (0.0538 g, 0.123 mmol) in nitromethane (20 mL) causing an immediate color change to dark red. The resulting solution was heated at reflux for 2 h, allowed to cool to room temperature, and the volume reduced to ~1/3 under reduced pressure. Diethyl ether vapor was diffused into the reaction solution yielding a dark red/orange crystalline solid (52.0 mg, 64%). Found C, 56.42; H, 3.64; N, 9.26%. $[Ag_2(C_{30}H_{22}N_4)_2](BF_4)_2.CH_3NO_2.H_2O$ requires: C, 56.18; H, 3.73; N, 9.51%). ^{1}H NMR (500 MHz, solvent, CD_3NO_2 [nitromethane-d_3] δ_H relative to CD_2HNO_2 at 4.33 ppm) 9.00 (4H, d, J = 7 Hz, H-b), 8.62 (4H, s, H-a), 7.66 (4H, d, J = 7 Hz, H-c), 7.61 (4H, t, J = 7 Hz, H-d), 7.45 (4H, t, J = 7 Hz, H-e), 7.37 (4H, d, J = 8 Hz, H-f), 7.12 (16H, m, H-g and H-h), 6.53 (4H, m, H-i). ^{13}C NMR (125 MHz, solvent CD_3NO_2 [nitromethane-d_3] δ_c relative to CD_3NO_2 at 62.81 ppm) 155.9, 155.8, 145.1, 138.4, 137.5, 134.6, 131.7, 131.0, 130.6, 129.2, 128.9, 121.5. IR (KBr disk, inter alia) ν_{max}/cm^{-1}: 3054 (m), 1618 (m), 1580 (m), 1558 (m), 1542 (s), 1475 (s), 1434 (s), 1071 (vs, br), 962 (m), 911 (m), 775 (m), 760 (s), 740 (s), 701 (s), 570 (m), 521 (m).

$[Ag_2(L^{m,m\text{-}Cl})_2](BF_4)_2\cdot 1/2(C_2H_5)_2O$. A solution of silver tetrafluoroborate (0.0246 g, 0.126 mmol) in nitromethane (5 mL) was added to a stirred yellow suspension of $L^{m,m\text{-}Cl}$ (0.0536 g, 0.126 mmol) in nitromethane (20 mL) causing an immediate color change to orange. The resulting solution was heated at reflux for 2 h, allowed to cool to room temperature, and the volume reduced to ~1/3 under reduced pressure. Diethyl ether vapor was diffused into the reaction solution yielding an orange crystalline solid (33.0 mg, 41%). Found C, 35.65; H, 1.67; N, 8.87%. $[Ag_2(C_{18}H_{10}Cl_4N_4)_2](BF_4)_2.{}^1/_2(C_2H_5)_2O$ requires: C, 35.81; H, 1.98; N, 8.79%). ^{1}H NMR (500 MHz, solvent, CD_3NO_2 [nitromethane-d_3] δ_H relative to CD_2HNO_2 at 4.33 ppm) 9.07 (4H, s, H-b), 8.64 (4H, s, H-a), 7.39 (4H, t, J = 1.8 Hz, H-d), 7.32 (8H, d, J = 1.7 Hz, H-c). ^{13}C NMR (125 MHz, solvent CD_3NO_2 [nitromethane-d_3] δ_c relative to CD_3NO_2 at 62.81 ppm) 161.1, 155.3, 152.0, 137.2, 136.1, 129.8, 121.9. IR (KBr disk, inter alia) ν_{max}/cm^{-1}: 3068 (m), 1621 (m), 1567 (vs), 1429 (s), 1051 (vs, br), 955 (s), 892 (m), 855 (s), 809 (s), 671 (m), 597 (m), 521 (m).

Results and Discussion

Synthesis of Silver(I) Complexes. All of the 1:1 reactions of $AgBF_4$ with the ligand of interest were carried out in the noncoordinating solvent nitromethane at reflux and generated products of stoichiometry $[Ag_nL_n](BF_4)_n\cdot solvent(s)$. In the case of $[Ag_n(L^{p\text{-}OH})_n](BF_4)_n$ the complex precipitated as an orange crystalline solid upon cooling the reaction mixture to room temperature, and was simply filtered off. For the other four new complexes, $[Ag_4(L^{p\text{-}Me})_4](BF_4)_4\cdot 2H_2O$, $[Ag_2(L^{o,p\text{-}Me})_2](BF_4)_2\cdot CH_3NO_2$, $[Ag_2(L^{o\text{-}Ph})_2](BF_4)_2\cdot CH_3NO_2\cdot H_2O$, $[Ag_2(L^{m,m\text{-}Cl})_2](BF_4)_2\cdot 1/2(C_2H_5)_2O$, the product was isolated as an orange-to-red solid by vapor diffusion of diethyl ether into the reaction solution after it was first reduced in volume by about a third. The yields were in the range 31−71%. The architecture of the product, dinuclear side-by-side vs tetranuclear [2 × 2] grid, and hence the value of n as indicated above, was established by single crystal X-ray structure determinations (see below) in all cases except for $[Ag_n(L^{p\text{-}OH})_n](BF_4)_n$, which resisted all attempts at crystallization.

All seven complexes (the five new complexes, plus the two complexes reported previously[11]) showed the expected imine stretches between 1618 and 1627 cm^{-1}, similar to those observed for the free ligands (1617−1625 cm^{-1}), and slightly higher than those observed for the analogous copper(I) complexes (range observed for the well resolved imine bands: 1613−1617 cm^{-1}).[3]

As was the case for the copper(I) complexes of these ligands,[3] no elucidation of the solution species, side-by-side dinuclear or [2 × 2] grid tetranuclear species, was possible by ES-MS as all of these silver(I) complexes fragmented extensively.

As in the study of the family of copper(I) complexes of these ligands,[3] attempts were made to access mixed ligand silver(I) complexes. These attempts included routes starting from either two preformed silver(I) complexes or from two free ligands and adding an equimolar amount of silver(I). Specifically, the following were tried: (a) mixing a 1:1 ratio of $L^{o,o,p\text{-}Me}$ and $L^{m,m\text{-}Cl}$ with 2 equiv of silver(I), (b) mixing a 1:1 ratio of silver complexes of $L^{p\text{-}OMe}$ and $L^{m,m\text{-}Cl}$, (c) mixing a 1:1 ratio of the

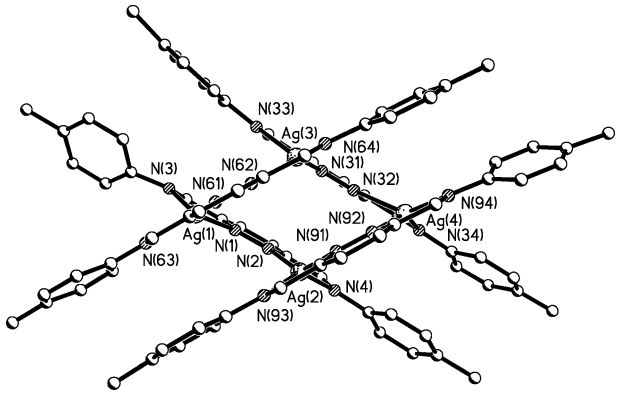

Figure 3. Perspective view of the $[Ag^{I}_4(\mathbf{L}^{p\text{-}Me})_4]^{4+}$ cation (hydrogen atoms omitted for clarity).

silver complexes of $\mathbf{L}^{o,o,p\text{-}Me}$ and $\mathbf{L}^{m,m\text{-}Cl}$. In no case was a clean product obtained from these reactions. A probe of a reaction carried out in deuterated nitromethane, by ^{1}H NMR spectroscopy, indicated that in solution a complex mixture of species was present, possibly including some mixed ligand complexes. However, the apparent lack of a clear thermodynamic sink led us to abandon our attempts to access mixed ligand silver(I) complexes.

X-ray Crystal Structures. Crystals of the silver(I) tetrafluoroborate complexes of ligands $\mathbf{L}^{p\text{-}OMe}$, $\mathbf{L}^{p\text{-}Me}$, $\mathbf{L}^{o,p\text{-}Me}$, $\mathbf{L}^{o\text{-}Ph}$, and $\mathbf{L}^{m,m\text{-}Cl}$ were isolated by a variety of methods, and the X-ray crystal structures were determined (Figures 3−6, Tables 1−3, Tables S3−S7, Supporting Information). The diffusion of diethyl ether vapor into a dimethylformamide solution of the appropriate complex gave single crystals of $[Ag_4(\mathbf{L}^{p\text{-}Me})_4](BF_4)_4\cdot 4.2[(CH_3)_2NCHO]\cdot 0.8[(C_2H_5)_2O]$ and twinned crystals of $[Ag_2(\mathbf{L}^{o\text{-}Ph})_2](BF_4)_2$. Single crystals of $[Ag_2(\mathbf{L}^{o,p\text{-}Me})_2](BF_4)_2\cdot CH_3NO_2$ were obtained by the diffusion of diethyl ether vapor into a nitromethane solution of the complex. Single crystals of $[Ag_2(\mathbf{L}^{m,m\text{-}Cl})_2](BF_4)_2\cdot C_6H_6\cdot 2CH_3NO_2$ and twinned crystals of $[Ag_4(\mathbf{L}^{p\text{-}OMe})_4](BF_4)_4\cdot 1.5C_6H_6\cdot$*solvent* (where *solvent* is the badly disordered solvents of crystallization that were dealt with by SQUEEZE; includes numerous further benzene molecules) were obtained by layering a nitromethane solution of the appropriate complex with benzene. Attempts to obtain crystals of the rather insoluble $[Ag_n(\mathbf{L}^{p\text{-}OH})_n]_n(BF_4)_n$ complex either by slow evaporation of the reaction filtrate or by diethyl ether vapor diffusion into a DMSO solution failed. Because of time constraints an attempt to grow crystals by slowly diffusing the reagents together was not carried out.

Both in the presence and in the absence[11] of benzene of solvation the silver(I) complex of $\mathbf{L}^{p\text{-}OMe}$ formed a [2 × 2] grid of four silver(I) ions with distorted tetrahedral coordination spheres (Figure S1, Supporting Information). Likewise, the silver(I) complex of $\mathbf{L}^{p\text{-}Me}$ formed a [2 × 2] grid (Figure 3). To the best of our knowledge (CSD version 5.25)[20] these are only the third and fourth single crystal structure determinations reported for [2 × 2] silver grids.[12,21] In contrast, the architectures of the silver(I) complexes with $\mathbf{L}^{o,p\text{-}Me}$, $\mathbf{L}^{o\text{-}Ph}$, and $\mathbf{L}^{m,m\text{-}Cl}$ are dinuclear side-by-side structures with the silver(I) ions adopting distorted square planar geometries (Figures 4−6, Figures S2−S3 Supporting Information), albeit with some additional interactions in the axial sites, similar to those seen previously in the silver(I) complex with $\mathbf{L}^{o,o,p\text{-}Me}$ (Figure S4, Supporting Information).[11]

Intramolecular Features. There is no crystallographically imposed symmetry within the [2 × 2] grids in either $[Ag_4(\mathbf{L}^{p\text{-}Me})_4](BF_4)_4\cdot 4.2[(CH_3)_2NCHO]\cdot 0.8[(C_2H_5)_2O]$ or the twinned, SQUEEZEd[19] structure $[Ag_4(\mathbf{L}^{p\text{-}OMe})_4](BF_4)_4\cdot 1.5C_6H_6\cdot$*solvent* (Figures 3 and S1). Indeed, in the latter structure two complete, crystallographically distinct and structurally different, tetranuclear grids are present in the asymmetric unit (Figure S1, Supporting Information): both grids are rhombically distorted, as evidenced by the angles between the neighboring, almost perpendicular, pyridazine rings deviating significantly from 90° [Ag(1)−Ag(4) grid 108.8−112.3°, Ag(5)−Ag(8) grid 111.8−112.0°] and the distinctly different diagonal Ag···Ag separations [Ag(1)−Ag(4) grid 4.823 and 6.216 Å, Ag(5)−Ag(8) grid 4.019 and 6.932 Å].[11] In the dinuclear side-by-side complex $[Ag_2(\mathbf{L}^{o,p\text{-}Me})_2](BF_4)_2\cdot CH_3NO_2$ there is only one silver ion and one ligand in the asymmetric unit, with the other half of the complex generated by inversion (Figure 4). The asymmetric unit of the twinned structure of $[Ag_2(\mathbf{L}^{o\text{-}Ph})_2](BF_4)_2$ contains two half complexes (two silver ions of different complexes, each of which binds two half ligands) with the other half of each complex generated by 2-fold rotation (Figures 5 and S2). The asymmetric unit of the side-by-side dinuclear complex $[Ag_2?>(\mathbf{L}^{m,m\text{-}Cl})_2](BF_4)_2\cdot C_6H_6\cdot 2CH_3NO_2$ also contains two half complexes, but in this case each consists of one silver ion and one complete ligand strand, and inversion generates the other half of each complex (Figures 6 and S3).

In both of the [2 × 2] grid complexes, all of the silver(I) ions have flattened tetrahedral geometries, with the sum of the N−Ag−N bond angles falling between 667(2)−671(3)° in $[Ag_4(\mathbf{L}^{p\text{-}OMe})_4]^{4+}$ and between 667(1)−672(1)° in $[Ag_4(\mathbf{L}^{p\text{-}Me})_4]^{4+}$. While these values and the average N−Ag−N angles of 111.6 and 111.5° are close to the ideal T_d values of 657° and 109.5°, respectively, the individual values range from 71.3(5)−144.3(5)° in $[Ag_4(\mathbf{L}^{p\text{-}OMe})_4]^{4+}$ and 71.5(2)−146.2(2)° in $[Ag_4(\mathbf{L}^{p\text{-}Me})_4]^{4+}$ (Table 2), far from the ideal T_d value of 109.5°. As expected, and as previously observed,[3,11] there is significantly greater deviation from ideal tetrahedral behavior in individual angles in the silver(I) grids than in the analogous copper(I) grids (individual bond angles 80.71(19)−138.68(8)°, sum of N−Cu−N bond angles = 662(2)−664(1)°, average bond angle = 110.6°).[2,3]

The sum of the N−Ag−N bond angles for the dinuclear side-by-side complexes of both $\mathbf{L}^{o,p\text{-}Me}$ and $\mathbf{L}^{m,m\text{-}Cl}$, 693(1)°, is closer to the ideal square planar value of 720° than to the tetrahedral ideal of 657° (Table 2). However, it should be noted that the situation is made more complicated for the $\mathbf{L}^{o,p\text{-}Me}$ complex as it also forms a weaker, fifth bonding interaction to a BF_4 anion [Ag−F = 2.7493 (18) Å; leading to a square pyramidal distortion of the Ag centers]. For the $\mathbf{L}^{m,m\text{-}Cl}$ complex there are also some reasonably close

(20) Allen, F. H. *Acta Crystallogr., Sect. B* **2002**, *58*, 380–388.
(21) Weissbuch, I.; Baxter, P. N. W.; Kuzmenko, I.; Cohen, H.; Cohen, S.; Kjaer, K.; Howes, P. B.; Als-Nielsen, J.; Lehn, J.-M.; Leiserowitz, L.; Lahav, M. *Chem. Eur. J.* **2000**, *6* (4), 725–734.

Table 2. Ranges of Metal Atom Bond Lengths and Angles for $Ag^{I}_4(\mathbf{L}^{p\text{-}OMe})_4]^{4+}$ Crystallized in Presence of Benzene, $[Ag^{I}_4(\mathbf{L}^{p\text{-}Me})_4]^{4+}$, $[Ag^{I}_2(\mathbf{L}^{o,p\text{-}Me})_2]^{2+}$, $[Ag^{I}_2(\mathbf{L}^{m,m\text{-}Cl})_2]^{2+}$, and $Ag^{I}_2(\mathbf{L}^{o\text{-}Ph})_2]^{2+}$ [a]

	$[Ag^{I}_4(\mathbf{L}^{p\text{-}Me})_4]^{4+}$	$Ag^{I}_4(\mathbf{L}^{p\text{-}OMe})_4]^{4+}$ crystallized in presence of benzene	$[Ag^{I}_2(\mathbf{L}^{m,m\text{-}Cl})_2]^{2+}$ [b]	$[Ag^{I}_2(\mathbf{L}^{o,p\text{-}Me})_2]^{2+}$ [c]	$[Ag^{I}_2(\mathbf{L}^{o\text{-}Ph})_2]^{2+}$ [d]	$Ag^{I}_4(\mathbf{L}^{p\text{-}OMe})_4]^{4+}$ without benzene[11]	$[Ag^{I}_2(\mathbf{L}^{o,o,p\text{-}Me})_2]^{2+}$ [11e]
Ag−N (Å)							
all Ag−N	2.288(5)−2.444(6)	2.217(11)−2.387(11)	2.301(6)−2.436(6)	2.317(2)−2.496(2)	2.326(4)−2.460(4)	2.275(6)−2.355(6)	2.298(3)−2.487(3)
(average)	(2.330)	(2.317)	(2.364)	(2.406)	(2.388)	(2.311)	(2.311)
$Ag-N_{pyridazine}$	2.292(5)−2.444(6)	2.217(11)−2.387(11)	2.301(6)−2.403(6)	2.317(2), 2.496(2)	2.432(5)−2.460(4)	2.275(6)−2.340(7)	2.298(3)−2.374(3)
(average)	(2.341)	(2.313)	(2.354)	(2.407)	(2.441)	(2.304)	(2.336)
$Ag-N_{imine}$	2.288(5)−2.368(6)	2.244(11)−2.360(14)	2.328(6)−2.436(6)	2.319(2),2.493(2)	2.326(4)−2.350(4)	2.287(6)−2.355(6)	2.365(3)−2.487(3)
(average)	(2.319)	(2.320)	(2.374)	(2.406)	(2.334)	(2.318)	(2.426)
N−Ag−N (°)							
distorted T_d− N−Ag−N	71.5(2)−146.2(2)	69.8(4)−145.1(5)				71.5(2)-144.2(2) (114.38)	
(average)	(111.6)	(111.5)					
cis-N−Ag−N			71.2(2)−113.2(2)	70.61(7)−111.3(7)	68.76(14)−132.40(11)		71.21(11)−116.02(11)
(average)			(91.0)	(89.9)	(92.2)		(90.7)
trans-N−Ag−N			159.3−170.0	155.49(6), 177.79(6)	151.66(15)−153.25(15)		163.69(12)−168.24(11)
(average)			(164.4)	(166.6)	(152.3)		(165.9)
Σ(N−Ag−N)	666.8−671.5	667.4−671.1	692.8, 692.9	693.0	673.1, 674.0	666.6−670.0	694.8
(average)	(669.7)	(669.0)	(692.9)		(673.6)	(668.7)	

[a] Also shown are the values for $Ag^{I}_4(\mathbf{L}^{p\text{-}OMe})_4]^{4+}$ crystallized without benzene,[11] and $[Ag^{I}_2(\mathbf{L}^{o,o,p\text{-}Me})_2]^{2+}$.[11] Mean values are given in parentheses. [b] This complex also contains a weaker, fifth bonding interaction to a benzene solvate, Ag−C = 3.23−3.36 Å. [c] This complex also contains a weaker, fifth bonding interaction to a tetrafluoroborate anion, Ag−F = 2.7493(18) Å. [d] This complex also contains a weak, fifth bonding η^2 interaction with the ligand's phenyl ring, Ag−C = 2.98 − 3.04 Å. [e] This complex also contains a weaker, fifth bonding interaction to a tetrafluoroborate anion, Ag−F = 2.920(3) Å.

Table 3. Comparison of Geometries from the X-ray Structural Data for $[Ag_4(\mathbf{L}^{p\text{-}Me})_4]^{4+}$, $[Ag_4(\mathbf{L}^{p\text{-}OMe})_4]^{4+}$, $[Ag_2(\mathbf{L}^{o,p\text{-}Me})_2]^{2+}$, $[Ag_2(\mathbf{L}^{m,m\text{-}Cl})_2]^{2+}$ and $[Ag_2(\mathbf{L}^{o\text{-}Ph})_2]^{2+}$

complex	$[Ag_4(\mathbf{L}^{p\text{-}Me})_4]^{4+}$	$[Ag_4(\mathbf{L}^{p\text{-}OMe})_4]^{4+}$	$[Ag_2(\mathbf{L}^{o,p\text{-}Me})_2]^{2+}$	$[Ag_2(\mathbf{L}^{m,m\text{-}Cl})_2]^{2+}$	$[Ag_2(\mathbf{L}^{o\text{-}Ph})_2]^{2+}$
Ag···Ag (Å) [a]	3.970−4.185	3.896−4.105	4.183	3.935, 3.940	4.398, 4.398
pyridazine to phenyl ring (<)°	5.9−23.2 (48.1)[b]	0.5−16.8	43.2, 57.3	40.2−46.2	19.5−22.8
pyridazine ring pairs					
number of ring pairs	2	4	0	0	0
mean plane angles (°)	1.0, 2.8	0.7−4.8			
centroid to centroid (Å)	3.61, 4.40	3.50−4.53			
mean plane to centroid (Å)	3.28−3.39	3.28−3.49			
offset angles (°)	20.1−40.8	15.2−38.4			
					pyridazine−phenyl pairs[d]
phenyl ring pairs					
number of ring pairs	4[c] (1)[b]	8	1	2	4
mean plane angles (°)	3.3−12.8 (47.5)[b]	5.8−12.1	14.2	9.6, 14.0	13.0−13.9
centroid to centroid (Å)	3.83−4.64 (4.38)[b]	3.73−4.61	3.97	3.79, 3.94	3.97−4.02
mean plane to centroid (Å)	3.31−3.67 (1.57, 4.75)[b]	3.39−3.65	3.32, 3.75	3.40−3.52	3.02−3.57
offset angles (°)	20.2−44.6 (23.9, 70.7)[b]	16.6−41.4	19.0, 33.1	22.0−27.5	26.6−41.1

[a] Ag···Ag distance for the pyridazine-bridged silver centers. [b] This atypical ring pair involves the higher occupancy site (sof = 0.8) of a disordered phenyl ring (C8−C13). [c] One of these four ring pairs involves the lower occupancy site (sof = 0.2) of a disordered phenyl ring (C8a−C13a). [d] This complex does not feature phenyl ring pair interactions, but does feature close phenyl-pyridazine contacts. These are probably not true π-π interactions, but rather occur due to the pyridazine's proximity to a silver ion, with which the phenyl ring is interacting, as discussed in the text.

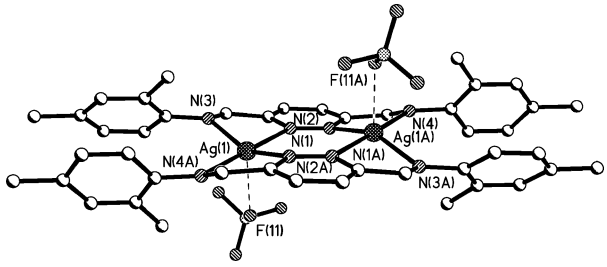

Figure 4. Perspective view of the $[Ag^{I}_2(\mathbf{L}^{o,p\text{-}Me})_2]^{2+}$ cation (hydrogen atoms omitted for clarity) and the weak axial interactions with the tetrafluroborate anions. The nitromethane molecules of solvation are not shown. Symmetry transformation used to generate equivalent atoms: $A = 1 - x, 1 - y, -z$.

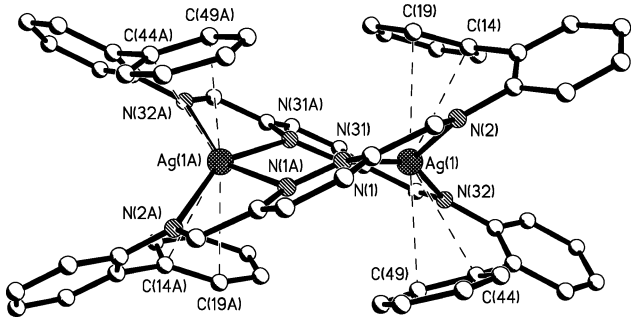

Figure 5. Perspective view of one of the two independent $[Ag^{I}_2(\mathbf{L}^{o\text{-}Ph})_2]^{2+}$ cations (hydrogen atoms omitted for clarity). Symmetry transformation used to generate equivalent atoms: $A = 1 - x, +y, 1.5 - z$.

Ag−$C_{benzene}$ contacts [Ag(1)−C(60)/C(62) and Ag(2)−C(70)/C(71): 3.23−3.36 Å]. The average *cis* angles, 89.9 and 91.0°, are very close to the square planar ideal (90°), but the average *trans* angles, 166.6 and 164.4°, are further from ideal (180°). The individual bond angles are quite widely dispersed: *cis* angles range 70.6−113.2° and *trans* angles range 155.5−177.8°. The side-by-side disilver(I) complex of $\mathbf{L}^{o\text{-}Ph}$ is somewhat different from these two side-by-side complexes: whereas the silver ions in the complexes of $\mathbf{L}^{o,p\text{-}Me}$ and $\mathbf{L}^{m,m\text{-}Cl}$ are relatively in-plane with respect to the pyridazine rings (silver

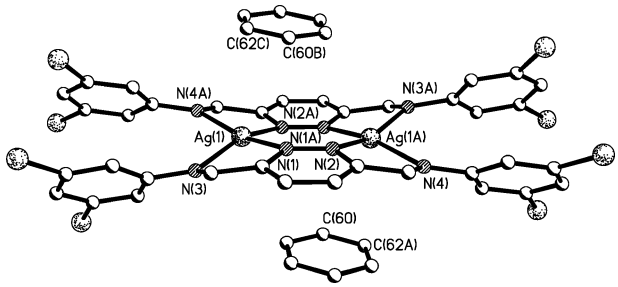

Figure 6. Perspective view of one of the two independent $[Ag^{I}_2(\mathbf{L}^{m,m\text{-Cl}})_2]^{2+}$ cations (hydrogen atoms omitted for clarity) and the associated benzene of solvation. Symmetry transformation used to generate equivalent atoms: $A = 1 - x, 1 - y, 1 - z$.

ion−pyridazine mean plane distances are 0.26−0.48 Å), the silver ions in $[Ag_2(\mathbf{L}^{o\text{-Ph}})_2]^{2+}$ lie well above/below the pyridazine ring mean plane (0.90−0.95 Å). This allows the *ortho*-phenyl rings to sandwich the silver ions, forming weak η^2 bonds[22] using the C bonded to the other phenyl ring, and one of the carbons adjacent to this [Ag(1)-C(14,19,44,49) = 2.98−3.04 Å]. This gives this complex a helical structure, as was previously observed in the copper(I) complex of this ligand[3] (Figure S5, Supporting Information). The sums of N−Ag−N bond angles for each of the two silver(I) ions in the asymmetric unit, 673(1) and 674(1)°, are closer to the tetrahedral than to the square planar value, but the additional interactions between the silver(I) ions and the *ortho*-phenyl rings clearly complicate the situation. Bond lengths are generally longer in the dinuclear complexes than the tetranuclear grids (average Ag−N bond lengths: grids, 2.323 Å; dinuclear, 2.386 Å). However, this analysis is complicated by the fact that all three dinuclear complexes have a fifth, weaker bonding interaction (either to a phenyl ring, BF_4 anion, or benzene solvate), causing the four Ag−N bonds to be longer. Generally Ag−imine and Ag−pyridazine bond lengths are very similar in length (average Ag−imine bond is within 0.022 Å of the average Ag−pyridazine bond) with the exception of the silver(I) complex of $\mathbf{L}^{o\text{-Ph}}$, in which the average Ag-pyridazine bond is 0.107 Å longer than the average Ag-imine bond, due to the silver-phenyl bond "pulling" the silver ion toward the imine nitrogen and away from the pyridazine ring.

Each of the ligand strands in the [2 × 2] grid molecules retains a reasonably planar conformation (Table 3), with the only phenyl-pyridazine twist angle of greater than 24° occurring for the higher occupancy (0.8) component of a disordered phenyl ring in $[Ag_4(\mathbf{L}^{p\text{-Me}})_4]^{4+}$. This disordered phenyl ring has a twist angle to the pyridazine ring of 48.1(4)°, thereby creating space to accommodate a 0.8 occupancy diethyl ether molecule of solvation. By definition, [2 × 2] grids have two pairs of roughly parallel ligand strands which are at right angles to one another. When the ligand contains aromatic groups π-π interactions between the parallel ligand strands in a pair can be anticipated. In both the $[Ag_4(\mathbf{L}^{p\text{-OMe}})_4]^{4+}$ and $[Ag_4(\mathbf{L}^{p\text{-Me}})_4]^{4+}$ [2 × 2] grids a series of interactions are present, between the almost parallel pairs of central pyridazine rings and also between the almost parallel pairs of terminal phenyl rings. Within each of the six pyridazine ring pairs the pyridazine rings are very close, within 5°, to parallel to each other (Table 3). They are significantly more offset from one another (mean plane−centroid distances 3.27−3.49 Å, centroid−centroid distances 3.50−4.33 Å, offset angles 15.2−40.8°) than was the case for the analogous copper(I) grids (copper mean plane−centroid distances 3.25−3.66 Å, centroid−centroid distances 3.61−3.91 Å, offset angles 12.5−33.2°). Calculations suggest that these pyridazine−pyridazine interactions are the least favorable intramolecular interactions present in these complexes (see later). Each terminal phenyl ring has a weak π-π interaction with the respective phenyl ring on the almost parallel ligand strand. Within each of the 12 phenyl ring pairs the phenyl rings are close, within 12.8°, to parallel to each other, other than the previously mentioned disordered group which makes a pair with an angle of 47.5° (Table 3). The mean plane−centroid distances are 3.31−3.67 Å (excluding the previously mentioned disordered phenyl ring for which these values are 1.57 and 4.75 Å). The centroid−centroid distances are more variable, due to the wide range of phenyl ring−phenyl ring offsets (1.2−3.3 Å), a much larger range than observed in the copper(I) complexes of these ligands.[3]

In contrast to the retention of fairly planar ligand conformations in the tetranuclear [2 × 2] grid complexes $[Ag_4(\mathbf{L}^{p\text{-OMe}})_4]^{4+}$ and $[Ag_4(\mathbf{L}^{p\text{-Me}})_4]^{4+}$, the formation of dinuclear side-by-side complexes requires a twisted ligand conformation in order to avoid the terminal phenyl rings clashing. The twisted ligand conformation also facilitates $\pi-\pi$ interactions between the resulting pairs of close to parallel phenyl rings.As expected, the dinuclear complexes of $\mathbf{L}^{o,p\text{-Me}}$ and $\mathbf{L}^{m,m\text{-Cl}}$ show substantial pyridazine−phenyl twists (40.2−57.3°). Within each of the three phenyl ring pairs the phenyl rings are close, within 14.2°, to parallel to each other and are weakly π-stacked (centroid−centroid distances: 3.79−3.97 Å, Table 3).

In the side-by-side complex of $\mathbf{L}^{o\text{-Ph}}$, the pyridazine-phenyl twists are not as pronounced (mean plane intersects: 19.5−22.8°), and there are no significant $\pi-\pi$ interactions between these phenyl rings. Rather, the more distant *ortho*-phenyl-substituent interacts axially with the silver ion (see above) and weakly π-stacks with the pyridazine ring (centroid−centroid distances 3.97−4.02 Å; mean plane intersects 13.0−13.9°, Table 3).

Intermolecular Features. In addition to the intramolecular $\pi-\pi$ interactions, which are a feature of all of the above complexes, numerous weak intermolecular interactions are present. These are summarized below, with more detail provided in the Supporting Information.

An interesting set of intermolecular interactions is observed in the structure of $[Ag_4(\mathbf{L}^{p\text{-OMe}})_4]^{4+}$. Reasonably strong parallel offset π-stacking is seen between the methoxyphenyl rings in the two crystallographically independent grids in the asymmetric unit (centroid−centroid distance = 3.61 Å, mean plane intersect = 4.0°), leading to the formation of a pillar-like architecture (Figure S6, Supporting Information). Furthermore, two pyridazine rings in one of the grids (the higher numbered grid) show parallel offset $\pi-\pi$ interactions

(22) Lindeman, S. V.; Rathore, R.; Kochi, J. K. *Inorg. Chem.* **2000**, *39*, 5707–5716.

with two of the benzene molecules of solvation (centroid−centroid: 3.71−3.75 Å, 7.8−8.6°), and these are in turn involved in weak CH−π hydrogen bonds[23] with phenyl ring hydrogen atoms from another complex (C–H···centroid = 3.55−3.64 Å, ∠C−H···C = 147−148°). The third benzene molecule present has a weak C−H···O interaction with a methoxybenzene oxygen atom (3.34 Å, 127°). Further similar interactions may be present with other benzene molecules of solvation, but these were so highly disordered that they were removed (and the SQUEEZE procedure of PLATON[19] applied), suggesting that any such interaction is weak.

The two "typical" dinuclear complexes (of $\mathbf{L}^{o,p\text{-Me}}$ and $\mathbf{L}^{m,m\text{-Cl}}$) contain $\pi-\pi$ interactions between adjacent molecules. In $[Ag_2(\mathbf{L}^{o,p\text{-Me}})_2]^{2+}$, a pyridazine ring in one complex and a phenyl ring of an adjacent complex stack in a parallel offset manner (centroid−centroid = 3.56 Å, mean plane intersect 7.6°) leading to a step-like stacking arrangement (Figure S7, Supporting Information). $[Ag_2(\mathbf{L}^{m,m\text{-Cl}})_2]^{2+}$ features close $\pi-\pi$ contacts between a pyridazine ring and a benzene solvate, which then interacts with the pyridazine of an adjacent complex. This results in the molecules stacking in pillars along the *a*-axis (Figure S8, Supporting Information). However, the exact nature of this interaction is difficult to determine, as the benzene solvate is in close proximity to both the pyridazine ring (centroid−centroid distances: 3.66−3.67 Å, mean plane intersects 5.2−7.1°) and the silver ions (Ag(1)−C(60)/C(62) and Ag(2)−C(70)/C(71): 3.23−3.36 Å).

All of the structures are stabilized by hydrogen bonds, of varying strengths, between the hydrogen atom attached to the imino-carbon atom and tetrafluoroborate anions or solvent molecules (C–H···X = 2.76−3.59 Å, X = anion or solvent; for full details see Supporting Information). Anion-π interactions[24] are seen between tetrafluoroborate anions and coordinated pyridazine rings (F···centroid distances >2.83 Å; for full details see Supporting Informtion) in all of the structures apart from the complexes of $\mathbf{L}^{m,m\text{-Cl}}$ and of $\mathbf{L}^{o\text{-Ph}}$. In the case of $\mathbf{L}^{m,m\text{-Cl}}$ this is because a benzene solvate interacts with the silver(I) ion and pyridazine ring, blocking the access of the anion to the electron-poor pyridazine-π-ring. This is similar in the case of $\mathbf{L}^{o\text{-Ph}}$, except that the *ortho*-phenyl rings, instead of a benzene solvate, block access to the anion.

$\pi-\pi$ Stacking Calculations. Stacking energies for each pair of potentially $\pi-\pi$ stacked aromatic groups within each complex were investigated using XED2.8.[25] Accurate calculation of the contribution of van der Waals and desolvation effects is a challenge for computational methods,[26] but any significant differences between the $\pi-\pi$ stacking interactions in the different systems are more likely to come from electrostatic effects.[27] Thus we will consider only the electrostatic interactions that are generally well-represented by the XED2.8 force-field and restrict our discussion to the relative values of different stacking interactions.[28] None of the $\pi-\pi$ stacking interactions stabilize the complexes in a coulombic manner, and there are significant substituent effects. The pyridazine ring pairs are the least favorable interactions, and these occur only in the grids. The most favorable pair of phenyl rings is the closest to a T−π or C−H to π ring pair and is observed within the grid complex formed by $\mathbf{L}^{p\text{-Me}}$. The dichlorophenyl ring pairs, in the side-by-side complex of $\mathbf{L}^{m,m\text{-Cl}}$, are the next most favorable. Most of the stability in complex formation probably comes from forming the four Ag−N bonds (grids av. Ag−N = 2.323 Å vs side-by-side complexes av. Ag−N = 2.386 Å).

Discussion of Structural Outcomes. The $\mathbf{L}^{p\text{-Me}}$ and $\mathbf{L}^{p\text{-OMe}}$ ligands both lack bulky substituents, so the ligands themselves can adopt an approximately planar conformation, stabilized by conjugation. When complexed it is expected that, in the absence of more compelling factors, these ligands would prefer to retain their planarity, and hence the stabilizing effects of conjugation, so should prefer to form tetrasilver(I) [2 × 2] grid structures rather than disilver(I) side-by-side complexes in the solid state. This is observed, with both $[Ag_4(\mathbf{L}^{p\text{-Me}})_4](BF_4)_4$ and $[Ag_4(\mathbf{L}^{p\text{-OMe}})_4](BF_4)_4$[11] structurally characterized. Indeed tetranuclear [2 × 2] grids were also the outcome when copper(I) was complexed with these two ligands.[2,3] The $\mathbf{L}^{p\text{-OH}}$ ligand, which also lacks bulky substitutents, is expected to prefer to remain planar, but it features *para*-hydroxyl moieties which are, in principle, capable of either coordinating or hydrogen bonding. Unfortunately, the silver(I) complex $[Ag_n(\mathbf{L}^{p\text{-OH}})_n](BF_4)_n$ was poorly soluble and lacked crystallinity, so no single crystal structure determination or useful mass spectral data could be obtained. Hence, no conclusions could be drawn about the value of *n* or about its supramolecular architecture.

We previously showed that introducing steric bulk, in the form of methyl substituents, to both of the phenyl ring sites *ortho* to the imine nitrogen gave a ligand, $\mathbf{L}^{o,o,p\text{-Me}}$, which was forced to be severely twisted away from planar [crystal structure showed that the pyridazine ring to phenyl ring angles were 76.20(10)° and 79.01(11)°], disrupting the conjugation throughout the ligand strand.[3] Not surprisingly, when complexed with silver(I) this twisted ligand facilitated the formation of a dinuclear side-by-side complex, $[Ag_2(\mathbf{L}^{o,o,p\text{-Me}})_2](BF_4)_2$.[11] To further probe this, the $\mathbf{L}^{o,p\text{-Me}}$ ligand, where just one of the two phenyl ring sites *ortho* to the imine nitrogen has a methyl substituent, was examined. Interestingly, and somewhat to our surprise, when it was complexed with copper(I) a strained [2 × 2] grid, $[Cu_4(\mathbf{L}^{o,p\text{-Me}})_4](BF_4)_4$, resulted.[2,3] It was suggested that this occurs because copper(I) does not readily adopt the distorted square planar geometry required to form a side-by-side complex, and so forms the strained grid as this allows it to adopt a geometry closer to tetrahedral. In contrast, silver(I) is more flexible geometrically and this is clearly illustrated here as a dinuclear side-by-side architecture is observed for the silver(I) complex

(23) Hunter, C. A.; Sanders, J. K. M. *J. Am. Chem. Soc.* **1990**, *112*, 5525–5534.
(24) Schottel, B. L.; Chifotides, H. T.; Dunbar, K. R. *Chem. Soc. Rev.* **2008**, *37*, 68–83.
(25) Vinter, J. G. *J. Comput.-Aided Mol. Des.* **1996**, *10*, 417–426.
(26) Hunter, C. A. *Angew. Chem., Int. Ed.* **2004**, *43*, 5310–5324.
(27) Cockroft, S. L.; Hunter, C. A.; Lawson, K. R.; Perkins, J.; Urch, C. J. *J. Am. Chem. Soc.* **2005**, *127*, 8594–8595.
(28) Chessari, G.; Hunter, C. A.; Low, C. R. M.; Packer, M. J.; Vinter, J. G.; Zonta, C. *Chem. Eur. J.* **2002**, *8*, 2860–2867.

Table 4. Calculated Coulombic Component of the $\pi-\pi$ Stacking Energies[a] Obtained Using XED2.8[25]

complex	ring pair[b]	calculated energy (kcal mol^{-1})
$[Ag^{I}_4(\mathbf{L}^{p\text{-OMe}})_4]^{4+}$	pyr−pyr	+4.86 to +5.54 (5.31)
$[Ag^{I}_4(\mathbf{L}^{p\text{-OMe}})_4]^{4+}$	RPh−RPh	+0.51 to +1.69 (1.05)
$[Ag^{I}_2(\mathbf{L}^{m,m\text{-Cl}})_2]^{2+}$	RPh−RPh	+0.35, +0.46 (0.41)
$[Ag^{I}_2(\mathbf{L}^{o,p\text{-Me}})_2]^{2+}$	RPh−RPh	+2.47
$[Ag^{I}_2(\mathbf{L}^{o,o,p\text{-Me}})_2]^{2+}$	RPh−RPh	+2.00

[a] Mean values are given in parentheses. [b] pyr = pyridazine, RPh = substituted terminal phenyl rings.

of this ligand, $[Ag_2(\mathbf{L}^{o,p\text{-Me}})_2](BF_4)_2$. By adopting a distorted square-planar geometry, and side-by-side architecture, the silver(I) ions facilitate the release of the steric strain caused by the *ortho*-methyl substituent, by rotation around the imine nitrogen−phenyl bond.

The complex of $\mathbf{L}^{o\text{-Ph}}$ also gave a side-by-side complex, as expected given the sterically demanding nature of this group, and the previously observed side-by-side copper(I) complex of this ligand.[3]

Surprisingly, the complex of $\mathbf{L}^{m,m\text{-Cl}}$ adopts a side-by-side architecture, despite the lack of a group *ortho* to the imine carbon that would force a rotation around the nitrogen−phenyl bond. Indeed, in dramatic contrast to this result, the copper(I) complex of this ligand is a [2 × 2] grid.[3] This is the only ligand studied that contains groups *meta* to the imine nitrogen, so it is not possible to be sure why it has behaved so differently. Careful examination of the structural parameters relating to the phenyl ring pairs, and comparison of these parameters with those observed for the $\mathbf{L}^{o,p\text{-Me}}$ analogue, did not indicate any unusual splaying apart of these rings to minimize possible Cl···Cl dipole−dipole repulsions. In fact, the *m,m*-chloro-substituted phenyl rings are slightly less splayed than the *o,p*-methyl-substituted phenyl ring pairs. This is consistent with favorable van der Waals interactions occurring between these polarizable substituents (intramolecular Cl···Cl separations 3.73−4.14 Å).[29] This conclusion is further reinforced by the observation that there are many *intermolecular* Cl···Cl interactions and these Cl···Cl separations start at just 3.55 Å. Calculations show that the $\pi-\pi$ stacking of these chloro-substituted rings is the most favorable of any of the phenyl ring pairs studied (Table 4). The chloro groups are also far more electron-withdrawing than the substituents on any of the other ligands in this family and this may reduce the stabilizing value of conjugation for this ligand. If so, then twisting the ligand to form the side-by-side complex would result in less of a loss of conjugation stabilization than for the other ligands, and it would also strengthen the Ag−N interactions somewhat (the twist should reduce the electron withdrawal from the nitrogen donor atoms by the dichlorophenyl rings). Presumably these factors, along with the geometric flexibility of silver(I), facilitate the adoption of the side-by-side architecture, which is further favored by the absence of pyridazine−pyridazine interactions, as these are energetically the least favorable of all of the pairs investigated (Table 4). For copper(I) the [2 × 2] grid is favored as this allows the copper(I) ions to adopt a geometry closer to tetrahedral.

It was thought that the presence of benzene in the crystal lattice of $[Ag_2(\mathbf{L}^{m,m\text{-Cl}})_2]^{2+}$ may help to explain the surprise formation of a side-by-side structure, as there is a weak interaction between one of the two silver ions and the benzene solvate (Ag−C contacts: 3.23−3.36 Å), which would not be possible if the complex adopted a [2 × 2] grid structure. Similarly, another side-by-side complex, $[Ag_2(\mathbf{L}^{p\text{-OPh}})_2]^{2+}$ is stabilized by close silver−phenyl contacts, albeit within the ligand strand in that case. To investigate this further, the previously reported[11] [2 × 2] grid complex $[Ag_4(\mathbf{L}^{p\text{-OMe}})_4]^{4+}$ was recrystallized in the presence of benzene. The resulting crystals contained numerous benzene molecules of solvation, but none of these interacts with the silver ions and the complex still forms a [2 × 2] grid. While silver−phenyl interactions may play a part in directing the structure of these complexes, the formation of the $[Ag_4(\mathbf{L}^{p\text{-OMe}})_4]^{4+}$ grid even in the presence of benzene solvates clearly shows that they are not an overriding factor. Given the weakness of the silver−benzene interactions in $[Ag_2(\mathbf{L}^{m,m\text{-Cl}})_2]^{2+}$, it appears that these interactions, in themselves, are a relatively minor factor in determining the structure of this complex.

The side-by-side architecture is observed more often for the silver(I) complexes of these relatively rigid bis-bidentate ligands than it was in the analogous family of copper(I) complexes.[3] This occurs despite the longer Ag−N than Cu−N bond lengths, which might favor grids over side-by-side complexes by reducing the less favorable pyridazine−pyridazine stacking interactions. Presumably this is due to the greater plasticity of silver(I), which allows it to more readily adopt the distorted square-planar geometry required for the side-by-side architecture, whereas copper(I) prefers a tetrahedral geometry more strongly, which leads to the observation of [2 × 2] grids in all but one case, that of the most hindered ligand, $\mathbf{L}^{o\text{-Ph}}$.

NMR Spectroscopy. With the exception of $[Ag_n(\mathbf{L}^{p\text{-OH}})_n](BF_4)_n$ all of the silver complexes had good solubility in deuterated nitromethane. $[Ag_n(\mathbf{L}^{p\text{-OH}})_n](BF_4)_n$ was poorly soluble in all solvents with only slight solubility in deuterated dimethylformamide. The ^{1}H NMR spectrum obtained in that solvent was well resolved, but a ^{13}C NMR spectrum could not be readily obtained. However, due to the use of dimethylformamide-d_7 instead of nitromethane-d_3, the data obtained cannot be readily compared with that obtained for the other complexes. In all cases the ^{1}H NMR peaks were able to be assigned readily by a combination of integration and 2-dimensional techniques (COSY, HMBC, HSQC and NOESY). The *ortho* and *para* methyl peaks for $[Ag_2(\mathbf{L}^{o,p\text{-Me}})_2](BF_4)_2$ were assigned based on their similarity in position to those observed in the trimethyl complex $[Ag_2(\mathbf{L}^{o,o,p\text{-Me}})_2](BF_4)_2$. For $[Ag_4(\mathbf{L}^{p\text{-OMe}})_4](BF_4)_4\cdot H_2O$ and $[Ag_2(\mathbf{L}^{o\text{-Ph}})_2](BF_4)_2$ the H-b peak is split (coupling of 6 and 7 Hz, respectively). This may derive from coupling to ^{109,107}Ag as has been seen previously for a disilver(I) complex of a crypt prepared from 3,6-diformylpyridazine and tren [(tris-2-aminoethyl)amine].[30] It is unclear why this coupling is not observed in all cases.

(29) Bondi, A. *J. Phys. Chem.* **1964**, *68*, 441–451.

(30) Brooker, S.; Ewing, J. D.; Nelson, J. *Inorg. Chim. Acta* **2001**, *317*, 53–58.

Table 5. Summary of the ^{1}H NMR Peak Positions of H-a (Pyridazine) and H-b (Imine Carbon) in the Complexes[a]

complex	H-a	H-b	Hammett constant	
$[Ag_4(\mathbf{L}^{p\text{-OMe}})_4]^{4+}$	8.53	9.05	σ_{para}-OMe	−0.27
$[Ag_4(\mathbf{L}^{p\text{-Me}})_4]^{4+}$	8.59	9.10	σ_{para}-Me	−0.17
$[Ag_2(\mathbf{L}^{o,p\text{-Me}})_2]^{2+}$	8.55	8.86		
$[Ag_2(\mathbf{L}^{o,o,p\text{-Me}})_2]^{2+}$	8.49	8.72		
$[Ag_2(\mathbf{L}^{o\text{-Ph}})_2]^{2+}$	8.62	9.00		
$[Ag_2(\mathbf{L}^{m,m\text{-Cl}})_2]^{2+}$	8.64	9.07	σ_{meta}-Cl	0.37
$[Ag_n(\mathbf{L}^{p\text{-OH}})_n]^{n+}$	*8.71*[a]	*9.22*[a]	σ_{para}-OH	−0.37

[a] $[Ag_n(\mathbf{L}^{p\text{-OH}})_n](BF_4)_n$ in dimethylformamide-d_7, δ_H relative to $(CD_3)_2NCHO$ at 8.02 ppm;[b] all other complexes in nitromethane-d_3, δ_H relative to CD_2HNO_2 at 4.33 ppm. Hammett constants[31−33] for the *meta*- and *para*-substituted benzoic acids are included for comparison purposes. [b] The values for $[Ag_n(\mathbf{L}^{p\text{-OH}})_n]^{n+}$ are italicized, as they were obtained in a different solvent so cannot be readily compared.

Disappointingly, the NOESY spectra did not show any correlations corresponding to interactions between adjacent ligand strands, with all of the observed interactions reasonably explained by intraligand correlations. For all seven silver(I) complexes, within the ligand strand a close interaction is observed, between H-b, the hydrogen on the imine carbon, and H-c, the phenyl ring hydrogen *ortho* to the imine nitrogen. For $[Ag_2(\mathbf{L}^{o,p\text{-Me}})_2](BF_4)_2$, while the peaks for H-c and H-d overlap, it is still reasonable to assign the NOESY crosspeak to the same H-b to H-c interaction. Interestingly, in the NOESY spectrum of $[Ag_2(\mathbf{L}^{o,p\text{-Me}})_2](BF_4)_2$, no interactions were observed between H-b and H-g, the *ortho* methyl substituent on the phenyl ring, which strongly suggests that the phenyl group is not free to rotate about the $N-C_{phenyl}$ bond; that is, due to steric factors the methyl group is constrained to be approximately *trans* to the imine group. This is the conformation observed in the solid state (see above).

The positions of the H-a and H-b hydrogen signals for all of the complexes studied in deuterated nitromethane and deuterated dimethyl formamide are compared in Table 5, and Hammett constants[31−33] for the *meta*- and *para*- substituents shown (Hammett constants are not valid for *ortho*-substituted species due to the steric complications introduced).[34] There is some variation in the H-a peak values, which fall between 8.49 ppm for the $[Ag_2(\mathbf{L}^{o,o,p\text{-Me}})_2](BF_4)_2$ complex and 8.64 ppm for the $[Ag_2(\mathbf{L}^{p\text{-OPh}})_2](BF_4)_2$ complex. The H-b vary somewhat more, from 8.72 ppm for the $[Ag_2(\mathbf{L}^{o,o,p\text{-Me}})_2](BF_4)_2$ complex to 9.10 ppm for $[Ag_4(\mathbf{L}^{p\text{-Me}})_4](BF_4)_4$.

Both the H-a and H-b signals move steadily upfield as the number of methyl substituents is increased from one to two to three in the complexes of $\mathbf{L}^{p\text{-Me}}$, $\mathbf{L}^{o,p\text{-Me}}$, and $\mathbf{L}^{o,o,p\text{-Me}}$, respectively.

Of the two complexes that exist as a [2 × 2] grid conformation in the solid state ($[Ag_4(\mathbf{L}^{p\text{-OMe}})_4]^{4+}$ and $[Ag_4(\mathbf{L}^{p\text{-Me}})_4]^{4+}$), the complex with the more negative Hammett constant (i.e., more electron-donating substituent), $[Ag_4(\mathbf{L}^{p\text{-OMe}})_4]^{4+}$, shows more shielded H-a and H-b signals than $[Ag_4(\mathbf{L}^{p\text{-Me}})_4]^{4+}$, as expected. This is in accordance with previous results for the analogous copper(I) complexes that exist as [2 × 2] grids in the solid state.[3] $[Ag_2(\mathbf{L}^{m,m\text{-Cl}})_2]^{2+}$, which exists as a side-by-side complex in the solid state, does not fit this trend. However, the variations are small, and, due to the nonplanar nature of these ligands, the above analysis is expected to be rather too simplistic.

Conclusions

The $\pi-\pi$ stacking of pyridazine ring pairs, present in [2 × 2] grid architectures, is calculated to have very unfavorable electrostatics. This may go some way to explain the results seen by Constable and co-workers,[7,8] where a dinuclear side-by-side architecture, in which these interactions are absent, was observed in contrast with the expected [2 × 2] grid based on the predicted preference of silver(I) ions for a tetrahedral geometry. However, unlike the ligands employed by Constable and co-workers, for our ligands to form side-by-side architectures, planarity cannot be maintained throughout the ligand strand. To adopt such an architecture our ligands must twist such that the phenyl groups are rotated out of the pyridazine−diimine plane. This required disruption of conjugation within the ligand strand disfavors the formation of side-by-side complexes. Hence, it is not surprising that for the ligands that are planar and conjugated, $\mathbf{L}^{p\text{-OMe}}$ and $\mathbf{L}^{p\text{-Me}}$, [2 × 2] grids of silver(I) ions are observed. In contrast, the introduction of methyl groups to the phenyl rings *ortho* to the imine bond forces the free ligand to twist, disrupting the conjugation, and preorganizing it for the formation of side-by-side complexes when bound to the metal ions. This is illustrated by the formation of side-by-side complexes of the twisted ligands $\mathbf{L}^{o,o,p\text{-Me}}$, $\mathbf{L}^{o,p\text{-Me}}$, and $\mathbf{L}^{o\text{-Ph}}$. The surprising outcome was that the silver(I) complex of the dichloro ligand ($\mathbf{L}^{m,m\text{-Cl}}$) displays a dinuclear side-by-side architecture. A dinuclear side-by-side architecture avoids pyridazine−pyridazine interactions, which calculations show to be relatively unfavorable. It also requires a twisted ligand and, as this is the ligand with the most electron withdrawing substituents in this series, this is expected to strengthen the Ag−N interactions somewhat and to result in only a small loss of conjugation stabilization (compared with the other ligands). But probably most importantly, silver(I) is readily able to adopt a distorted square-planar geometry and hence the side-by-side architecture. This is in contrast to the copper(I) complex of this ligand, which is a [2 × 2] grid, presumably due to the increased preference of copper(I), over that of silver(I), for a tetrahedral geometry.

Acknowledgment. We thank Professor W. T. Robinson and Dr. J. Wikaira (University of Canterbury) for the X-ray data collections for $[Ag_2(\mathbf{L}^{o,p\text{-OMe}})_2][BF_4]_2$ and $[Ag_2(\mathbf{L}^{m,m\text{-Cl}})_2][BF_4]_2$. This work was supported by grants from the Marsden Fund (Royal Society of New Zealand; JRP & SB) and the University of Otago (NGW & SB).

Supporting Information Available: Crystallographic data in CIF format, X-ray crystal structure refinement and SQUEEZE details, additional views of packing, full details of intermolecular interactions and tables of silver ion bond lengths and angles. This material is available free of charge via the Internet at http://pubs.acs.org.

IC800959S

(31) Hammett, L. P. *Chem. Rev.* **1935**, *17*, 125–136.
(32) McDaniel, D. H.; Brown, H. C. *J. Org. Chem.* **1958**, *23*, 420–427.
(33) Hansch, C.; Leo, A.; Taft, R. W. *Chem. Rev.* **1991**, *91*, 165–195.
(34) Jaffé, H. H. *Chem. Rev.* **1953**, *53*, 191–260.